Electron. Mater. Lett., Vol. 11, No. 3 (2015), pp. 435-439
DOI: 10.1007/s13391-014-4457-z

Nano-Geometry Dependent Electrical Property of Organic Semiconductor

Bong-Gi Kim,[1] Uisik Kwon,[2] Dong Hyuk Park,[3,*] and Hui Joon Park[2,*]

[1]Department of Organic and Nano System Engineering, Konkuk University, Seoul 143-701, Korea
[2]Division of Energy Systems Research, Ajou University, Suwon 443-749, Korea
[3]Division of Nano-systems Engineering, Department of Applied Organic Materials Engineering, Inha University, Incheon 402-751, Korea

(received date: 9 December 2014 / accepted date: 13 December 2014 / published date: 10 May 2015)

In this work, we manipulated the crystallinity and geometry of P3HT nanodomains and investigated their effects on carrier mobility of organic thin film transistor (OTFT). Furthermore, it was confirmed that the reproducibility of OTFT devices could be improved with nanostructure-based active layer. P3HT nanostructures, nanodot and nanowire, were prepared through the control of polymer solution concentration and ultrasonic treatment. Those nanostructures produced well-organized crystalline morphology, which resulted in outperforming field-effect mobility, compared to bulk P3HT film, thermally annealed after spin-casting. OTFT devices fabricated with P3HT nanowires showed slightly higher electrical mobility than those with nanodots, due to their geometric advantage for inter-connection between electrodes. In terms of device-to-device uniformity, nanodot-based devices have lower performance variation among OTFT arrays due to their symmetric geometry.

Keywords: organic semiconductor, thin film transistor, nanostructure, geometry, reproducibility

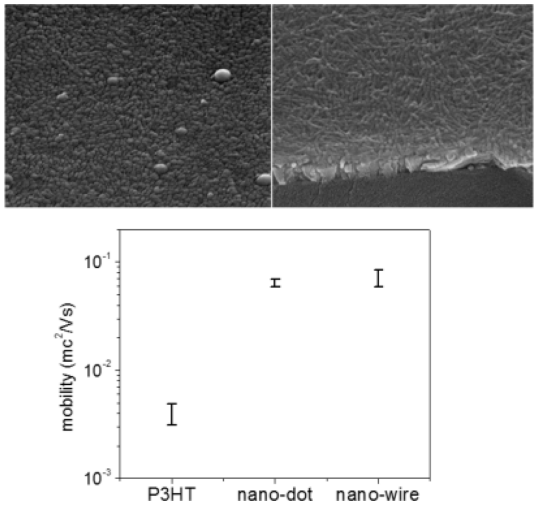

1. INTRODUCTION

Organic thin film transistor (OTFT) employing an organic material as a semiconducting active layer has been great attention due to the feasibility of simple fabrication process and the applicability to the flexible substrates.[1-6] In OTFT devices, it is well known that electrical properties of devices (e.g. carrier mobility) are significantly affected by the film morphology of organic semiconductors, mostly determined by their crystallization behavior.[7,8] Furthermore, achieving high device-to-device uniformity of performances is challenging because the film quality of active layer is strongly affected by the casting processes as well as the inherent crystallization behavior of organic semiconductors themselves, especially when prepared to a large area format. Therefore, designing effective processes that can give higher crystallinity, for better carrier mobility, and finding the correlation between aggregation behavior of molecules and device-to-device uniformity, for reproducibility of devices, are crucial steps to realize this technology in near future, which we are focusing on in this article.

Poly-3-hexylthiophene (P3HT) is one of the attractive semiconducting materials to investigate the effect of film morphology on the electrical properties such as carrier mobility because its crystallinity, affecting the film morphology, can be easily tuned by controlling region-regularity of polymer chain or applying different annealing processes.[7,9-11] In general, intermolecular charge transfer can be facilitated in crystalline region of P3HT through the strong π-π interaction, which results in outperforming field-effect mobility. To enhance the crystallinity, several film-forming techniques have been reported, such as thermal treatment,[9] spin casting with nonvolatile solvents,[10] surface pretreatment,[12] printing-based process,[13-15] and special tools for chain alignment.[16-18] The field-effect mobility obtained from these film fabrication techniques reached up

*Corresponding author: donghyuk@inha.ac.kr
*Corresponding author: huijoon@ajou.ac.kr

to 0.1 - 0.3 $cm^2/V \cdot s$. Especially, we have invented the solution-based in-situ process that can efficiently produce semiconductor polymer nanowires, consequently giving superior electrical properties when applied to organic photovoltaics.[19] Based on this approach, in this work, we manipulated the dimension of P3HT nanostructures and investigated their geometric effect on field-effect mobility. Furthermore, it was confirmed that the reproducibility of OTFT devices could be improved with nanostructure-based active layer.

2. EXPERIMENTAL PROCEDURE

2.1 Preparation of P3HT Nanostructures

91% regio-regular P3HT was purchased from Rieke Metals and used without further purification. In case of P3HT nanowire, 10 mg of P3HT was dissolved in chlorobenzene/acetonitrile co-solvent system (1.0 mL/0.07 mL), and the obtained orange color solution was treated with ultrasonication at room temperature for 2 minutes. The solution was kept under ambient condition for 2 hours to allow crystallization of P3HT in the solution state. Then, the solution was treated by ultrasonication again, to disassemble randomly entangled chains, and it was stored under ambient condition. The same procedure was repeated four times to improve the uniformity of P3HT nanowire. The resulting homogeneous suspension was spin-cast to form a thin layer film for further investigation. In case of P3HT nanodot, 1.0 mg of P3HT was applied to the same composition of co-solvent (1.07 mL), and ultrasonication was repeatedly treated as similarly as the preparation of P3HT nano-wire.

2.2 Organic Field-Effect Transistor (OFET) Device

Bottom-gate, top-contact field effect transistors (FETs) were fabricated to characterize electrical properties of obtained polymer films. After cleaning the silicon wafer in a Piranha solution, octadecyltrichlorosilane (OTS, water contact angle; 72°) was treated on thermally grown oxide surface (260 nm) and polymer films (80 nm) were prepared by means of spin coating method. Then, source and drain electrodes (Au, 100 nm) were thermally evaporated through shadow mask with channel width and length of 200 μm, and 100 μm, respectively. The field effect mobility was extracted from the saturation regime using the relationship, $\mu(\text{sat}) = (2I_{DS} \cdot L)/(W \cdot C \cdot (V_G - V_{th})^2)$, where I_{DS} is saturation drain current, C is capacitance (11 nF cm^{-2}) of dielectric layer (SiO_2), V_G is gate voltage, and V_{th} implies threshold voltage. The device performance was evaluated in air using Keithley 4200-SCS semiconductor analyzer.

3. RESULTS AND DISCUSSION

P3HT nanostructures were directly prepared through the ultrasonic treatment on P3HT solution and their dimension could be successfully controlled by changing the concentration of P3HT in solution. As illustrated in Fig. 1a, the film, spun with neat P3HT solution, has no characteristic morphology in SEM image, even after thermal treatment. On the contrary, quasi-spherical shaped nano-domains could be successfully prepared (Fig. 1b, nanodot) by spin-casting the ultrasonication-treated polymer solution, in which 1.0 mg P3HT was dissolved into chlorobenzene/acetonitrile cosolvent (1 mL/0.07 mL). Moreover, the length of P3HT nanodots could be increased to be nanowire type structures as the concentration of polymer solution increased from 1 mg to 10 mg (Fig. 1c). However, the diameter of nanowire was preserved to be 20 nm, the same dimension as nanodot. Since the field-effect carrier mobility is directly affected by the crystallinity of organic semiconductors in active layer of OTFT, firstly, the crystallinity of each film was investigated by UV-vis. absorption spectroscopy. It is well known that P3HT exhibits three vibronic absorption shoulders and they are much more pronounced as its crystallinity increases. As shown in Fig. 2, the thermally annealed spin-cast P3HT showed relatively weak absorption peaks around 556 nm (2^{nd} peak) and 610 nm (3^{rd} peak), which indicated that this approach was not strong enough to fully crystallize polymer chains. Compared to this, the films spun with ultrasonic-

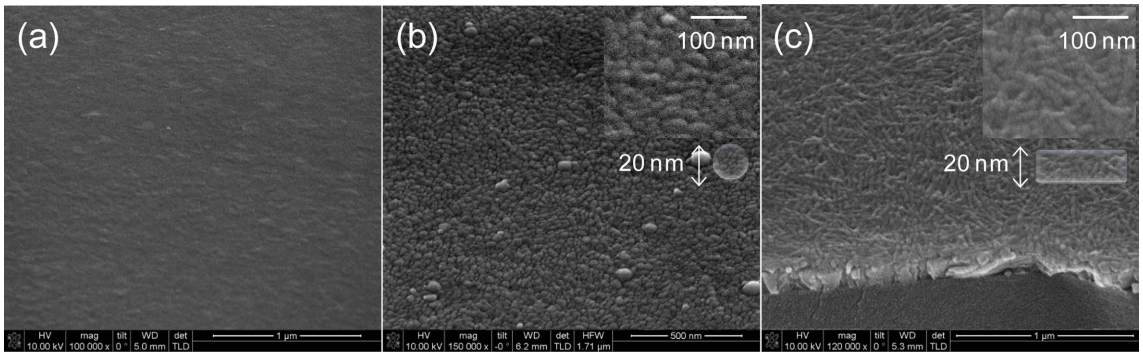

Fig. 1. SEM images of (a) thermally annealed P3HT film, (b) nanodot and (c) nanowire prepared by the ultrasonic-assisted self-assembly method.

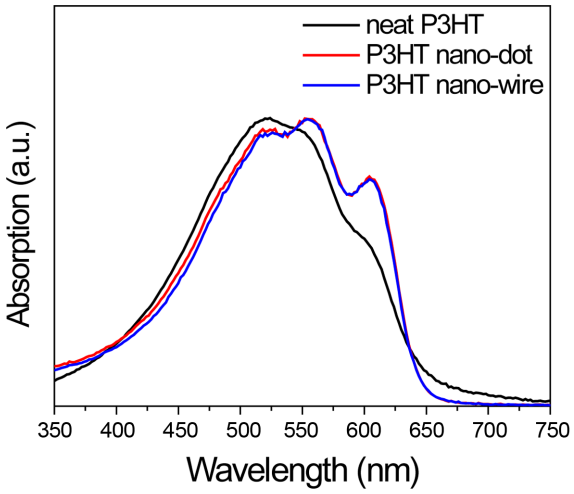

Fig. 2. UV-vis. absorption spectra of thermally annealed P3HT film, P3HT nanodot film and P3HT nanowire film.

treated P3HT solution exhibited significantly enhanced 2nd and 3rd absorption peaks, which meant a higher degree of ordering of polymer chains was achieved. Interestingly, both nanodot- and nanowire-based thin films showed almost the same absorption propensity, even though their geometry was noticeably dissimilar. From the fact that those nanostructures have the similar degree of polymer chain ordering and diameter, about 20 nm scale, we speculate that nanowires are grown from nanodots structure as the concentration of polymer solution increases.

Next, top-contact and bottom-gate FETs were fabricated to investigate the effect of nanomorphology of polymer semiconductors on carrier mobility. A heavily doped *n*-type Si/SiO_2 wafer was used as the substrate, wherein the conductive Si wafer and the surface SiO_2 layer (260 nm) function as the common gate electrode and the gate dielectric, respectively. The SiO_2 gate dielectric was treated with octadecyltrichlorosilane (OTS) to form a self-assembled monolayer (SAM), whereon P3HT solution was spun and thermally dried (120°C). Source and drain (Au, 100 nm) were then thermally evaporated through shadow mask, and the width (W) and the length (L) of channel were defined as 200 μm, and 100 μm, respectively. The FET carrier mobility was extracted from the saturation regime using the relationship, $\mu(\text{sat}) = (2I_{DS} \cdot L)/(W \cdot C \cdot (V_G - V_{th})^2)$, where I_{DS} is saturation drain current, C is capacitance (11 nF cm^{-2}) of dielectric layer (SiO_2), V_G is gate voltage, and V_{th} implies threshold voltage. The device performances were evaluated in air using Keithley 4200-SCS semiconductor analyzer. As illustrated in Fig. 3, the P3HT films containing nanostructures (nanodot or nanowire) exhibited much enhanced field-effect mobility. The carrier mobility of thermally annealed P3HT (Fig. 3a) was around 0.004 cm^2/(V·s), which is comparable to previously reported values,[4,20-22] whereas the mobility obtained with P3HT nanodot (Fig. 3b) and nanowire (Fig. 3c) reached up to 0.064 cm^2/(V·s) and 0.072 cm^2/(V·s), respectively. We believe that higher carrier mobility of

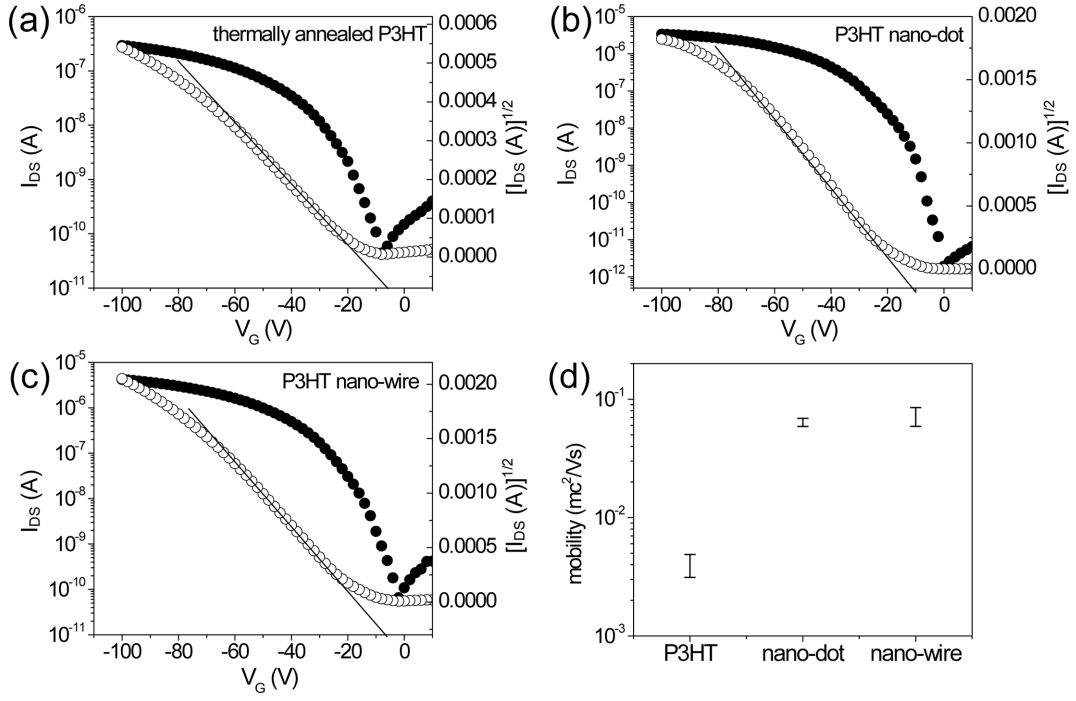

Fig. 3. Transfer curve of FET devices fabricated with (a) thermally annealed P3HT film, (b) P3HT nanodot, and (c) P3HT nanowire. The device-to-device uniformity of carrier mobility was summarized in (d).

nanostructured P3HT films would be mainly due to the enhanced crystallinity of polymer chains. Especially, slightly higher carrier mobility was shown in nanowire-based OTFTs, compared to that in nanodot type devices, and this extra gain came from the geometric effect of a wire-shaped nanostructure, which was more advantageous to channel formation between source and drain (100 μm).

Device-to-device uniformity is one of the essential factors for the commercialization of organic semiconductor-based TFT. To realize the devices having small device-to-device deviation, we have studied the effect of geometry of nanodomains on the performance of OTFT devices. For this purpose, OTFT arrays, composed of more than 50 unit cells, on 11.8-inch Si wafer were prepared. As illustrated in Fig. 3d, the carrier mobilities of thermally annealed spin-cast devices (data deviation of calculated mobility ~22%) and nanowire-based devices (~18%) showed relatively large variation, compared to those of nanodot-based devices (~8%). The large variation of mobilities in thermally annealed spin-cast devices could be due to the ununiformly developed crystalline domains on large area substrate, originated from the restricted migration of polymer chains in quickly dried film that prevented them from being efficiently organized, even under high temperature thermal annealing. As for nanostructured P3HT films, we believe that nanoscale structures (nanodot and nanowire), already uniformly formed during ultrasonic treatment in solution, can be efficiently spread out on large area by the shear force applied during spin-casting, consequently giving relatively lower performance deviation among devices. Especially, nanodot-based devices that have symmetric geometry show much lower performance deviation, because nanowire-based devices inevitably have anisotropic properties according to the direction of nanowires.[20] Our results suggest that pre-crystalized organic semiconductors that have symmetric nano-geometry such as nanodot would be helpful to achieve low device-to-device deviation as well as relatively high carrier mobility.

4. CONCLUSIONS

We prepared different types of nanostructures by controlling the concentration P3HT solution under ultrasonic treatment. Nanodot structures could be prepared from low concentration P3HT solution, and those nanodots grew up to the asymmetric nanowires as the concentration increased. Although these nanostructures have different geometry, their degree of chain ordering was similar as compared with UV-vis. absorption spectroscopy. To investigate the effects of both crystallinity and nano-geometry on the electrical property of organic semiconductors, we fabricated OTFT devices and compared their field-effect mobilities. Firstly, our results showed that OTFTs with the films, containing high crystalline P3HT nanodomains (nanodots and nanowires), exhibited much higher carrier mobilities than those with spin-casting-based thermally annealed films. Furthermore, those nanostructured devices also showed better device-to-device uniformity of carrier mobilities, which were calculated using OTFT arrays, composed of 50 cells. Among different types of nanostructures, nanowire type geometry was beneficial to efficient carrier transport due to their easy channel formation property, compared to nanodot type geometry, however, its anisotropic property was not very helpful to have good uniformity among devices. Consequently, nanodot-based devices showed reasonably high carrier mobility due to their high crystallinity and superior uniformity due to their symmetric geometry. We believe that our work would be helpful to design the nanomorphology of active layer in OTFTs, such as crystallinity and nano-geometry, to improve their performances and uniformity for a future flexible electronics technology.

ACKNOWLEDGEMENTS

HJP acknowledges the support by the Basic Science Research Program through the National Research Foundation of Korea (NRF) funded by the Ministry of Education (2014R1A1A2056403). DHP acknowledges the support by the Inha University Research Grant (Grant No. INHA-47291).

REFERENCES

1. Z. Bao, A. Dodabalapur, and A. J. Lovinger, *Appl. Phys. Lett.* **69**, 4108 (1996).
2. M. Kobashi and H. Takeuchi, *Macromolecules* **31**, 7273 (1998).
3. H. Sirringhaus, P. J. Brown, R. H. Friend, M. M. Nielsen, K. Bechgaard, B. M. W. Langeveld-Voss, A. J. H. Spiering, R. A. J. Janssen, E. W. Meijer, P. Herwig, and D. M. de Leeuw, *Nature* **401**, 685 (1999).
4. B.-G. Kim, E. J. Jeong, J. W. Chung, S. Seo, B. Koo, and J. Kim, *Nat. Mater.* **12**, 659 (2013).
5. Y. K. Lee, M. Maniruzzaman, C. Lee, M. J. Lee, E.-G. Lee, and J. Lee, *Electron. Mater. Lett.* **9**, 741 (2013).
6. S.-W. Lee, C.-H. Kim, S.-G. Lee, J.-H. Jeong, J.-H. Choi, E.-S. Lee, *Electron. Mater. Lett.* **9**, 471 (2013).
7. R. J. Kline, M. D. McGehee, E. N. Kadnikova, J. S. Liu, and J. M. J. Frechet, *Adv. Mater.* **15**, 1519 (2013).
8. R. Noriega, J. Rivnay, K. Vandewal, F. P. V. Koch, N. Stingelin, P. Smith, M. F. Toney, and A. Salleo, *Nat. Mater.* **12**, 1038 (2103).
9. S. Cho, K. Lee, J. Yuen, G. Wang, D. Moses, A.J. Heeger, M. Surin, and R. Lazzaroni, *J. Appl. Phys.* **100**, 114503 (2006).
10. J.-F. Chang, B. Sun, D. W. Breiby, M. M. Nielsen, T. I. Solling, M. Giles, I. M. Culloch, and H. Sirringhaus, *Chem. Mater.* **16**, 4772 (2004).

11. H. Yang, T. J. Shin, L. Yang, K. Cho, C. Y. Ryu, and Z. Bao, *Adv. Funct. Mater.* **15**, 671 (2005).
12. D. H. Kim, Y. D. Park, Y. Jang, H. Yang, Y. H. Kim, J. I. Han, D. G. Moon, S. Park, T. Chang, C. Chang, M. Joo, C. Y. Ryu, and K. Cho, *Adv. Funct. Mater.* **15**, 77 (2005).
13. H. J. Park, M.-G. Kang, S. H. Ahn, and L. J. Guo, *Adv. Mater.* **22**, E247 (2010).
14. H. J. Park, H. Kim, J. Y. Lee, T. Lee, and L. J. Guo, *Energy Environ. Sci.* **6**, 2203 (2013).
15. H. J. Park, J. Y. Lee, T. Lee, and L. J. Guo, *Adv. Energy Mater.* **3**, 1135 (2013).
16. G. Wang, J. Swensen, D. Moses, and A. J. Heeger, *J. Appl. Phys.* **93**, 6137 (2003).
17. S.-Y. Min, T.-S. Kim, B. J. Kim, H. Cho, Y.-Y. Noh, H. Yang, J. H. Cho, and T.-W. Lee, *Nature Commun*. **4**, 1773 (2013).
18. H. Cho, S.-Y. Min, and T.-W. Lee, *Macromol. Mater. Eng*. **298**, 475 (2013).
19. B.-G. Kim, M.-S. Kim, and J. Kim, *ACS Nano* **4**, 2160 (2010).
20. B. O'Connor, R. J. Kline, B. R. Conrad, L. J. Richter, D. Gundlach, M. F. Toney, and D. M. DeLongchamp, *Adv. Funct. Mater.* **21**, 3697 (2011).
21. H. R. Tseng, L. Ying, B. B. Y. Hsu, L. A. Perez, C. J. Takacs, G. C. Bazan, and A. J. Heeger, *Nano Lett.* **12**, 6353 (2012).
22. R. J. Li, L. Jiang, Q. Meng, J. H. Gao, H. X. Li, Q. X. Tang, M. He, W. P. Hu, Y. Q. Liu, and D. B. Zhu, *Adv. Mater.* **21**, 4492 (2009).